STATE REDUCED ORDER MODELS FOR THE MODELLING OF THE THERMAL BEHAVIOR OF BUILDINGS

Christophe Ménézo – menezo@insa-cethil-etb.insa-lyon.fr
CETHIL/Equipe Thermique du Bâtiment UMR CNRS 5008
INSA de Lyon – Bât. 307 – 20 Av. A. Einstein 69621 Villeurbanne Cedex – France
Hassan Bouia – bouia@insa-cethil-etb.insa-lyon.fr
Jean-Jacques Roux – roux@insa-cethil-etb.insa-lyon.fr
Patrick Depecker – depecker@insa-cethil-etb.insa-lyon.fr

Abstract. This work is devoted to the field of building physics and related to the reduction of heat conduction models. The aim is to enlarge the model libraries of heat and mass transfer codes through limiting the considerable dimensions reached by the numerical systems during the modelling process of a multizone building. We show that the balanced realization technique, specifically adapted to the coupling of reduced order models with the other thermal phenomena, turns out to be very efficient.

Keywords: Building Physics, System Reduction, Balanced realization, Experimental test

1. INTRODUCTION

Buildings are thermal systems with complex design and extended area. When modelling, the scales are depending upon either the interest in the energetic behavior of the whole building or in a particular dwelling zone. This system is submitted to numerous internal and external thermal impact factors that modify its state according to a large scale of times. The different mechanisms of heat transfer are clearly identified and an accurate modelling of each of them is mastered: heat conduction through the envelope, radiation, convection and heat transfers between zones connected with mass transfer. The main problem lies in the fact that these phenomena may vary according to an interrelated manner and, very often with the same impact. The modelling of all these interconnected phenomena still remains difficult to achieve: a reasonable balance between the expected accuracy of results and the computation times has to be maintained.

We present in this paper a reduction technique applied to conductive systems. The adopted way is based on a sub-structuring approach leading to an automatic generation of reduced order models, associated with elementary components of the envelope : 1D (multi-layer walls), 2D (complex walls, thermal bridges) or 3D (bonding building-ground). This work has been aimed towards performing (in transient rate) and practical (interface CAD) codes allowing Consulting Engineers to conceive and rapidly analyze the airflow-thermal behavior of buildings.

2. HEAT CONDUCTION MODELS

2.1 Considered systems

In buildings, four different heat transfer mechanisms evolve in a interconnected manner and, usually, with a similar importance: conduction, radiation, convection and mass transfer. The equations ruling the thermal evolution of this structure reflect the coupling of these phenomena through the energy conservation.

The conduction evolving within the envelope can only be reasonably described by laws which are both linear and time invariant. Mathematical developments allowed to express accurately these diffusion phenomena. However, the building envelope is a complex geometric domain made of many peculiarities. The thermal transfers are in fact at least 2D. Resorting to numerical methods implies a spatial discretization (Fig.1) of the heat equation and leads to a set of differential equations Eq.(1.a). They allowed to relate the evolution of the temperature field $T(M_i,t)$ of the n control volumes to the time varying p excitations gathered in vector $U(t)$. An observation equation (1.b) is associated with this system and enables to follow the evolution of a number q of observed variables set in the vector $Y(t)$.

$$\begin{cases} C_{apa}.\dot{T}(M_i,t) = A_0.T(M_i,t) + B_0.U(t) & \text{(1.a)} \\ Y(t) = C_0.T(M_i,t) + D.U(t) & \text{(1.b)} \end{cases}$$

C_{apa} is the matrix of the thermal capacities associated with each elementary volume i. This matrix is diagonal (Finite Differences or Finite Volumes) and is defined as positive. Matrix A_0 is made of the thermal conductivities linking the elementary volumes. This matrix has negative and dominant terms on its diagonal and is also symmetric. B_0 is the matrix of the driving forces. C_0 is the observation matrix and D the direct transmission matrix.

Besides, it is important to highlight that this type of model is built in order to carry out afterwards the coupling with the other thermal phenomena. For this reason, the p-outputs (fluxes led on the surfaces : Φ_{cond}) are observed on the boundaries of each envelope component where the q-exitations (surface temperatures : Ts) are applied too. Consequently, there are as many observed variables than of excitation variables : $p = q$. The excitation matrix B_0 and the matrix of observation C_0 are thus made with the same thermal conductivities and are equal in transposed : $B_0^T = C_0$. This is very interesting for the use of the reduction technique called balanced realization suggested by Moore (1981).
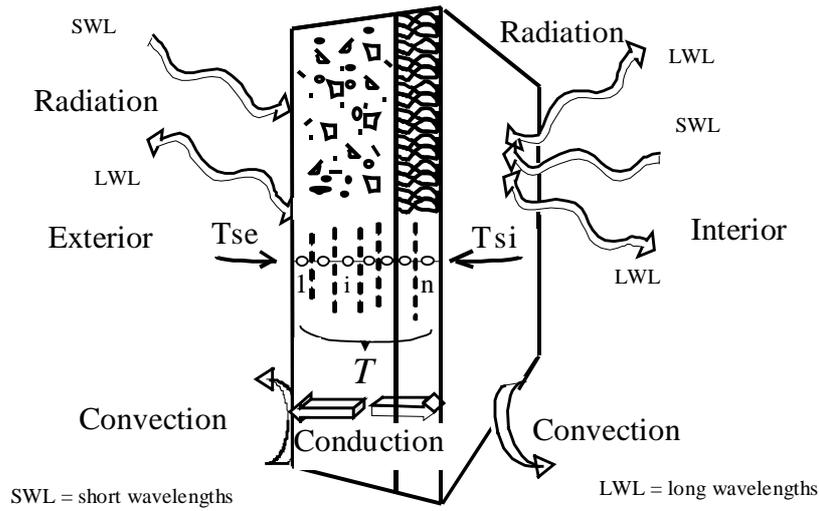
Figure 1- Control volumes for an elementary component of the envelope and boundary conditions

2.2 Adapted balanced realization technique

The dimension of system Eq.(1) depends on the mesh accuracy. It can increase considerably for a multizone building. So, it is necessary to reduce the set of differential equations.

The methods related to the reduction of invariant linear systems consist in selecting r variables among the n state variables of the system. These variables are considered as preponderant for the model evolution. The aim is to achieve a reduced model of order $r \ll n$ which reproduces the most accurate dynamic behavior. The formulation of the original detailed model Eq.(1) and the selection criteria differ with the method.

We present first the chosen initial formulation before dwelling on Moore's technique: the balanced modal form. This formulation enables (see *infra*) to reduce quite considerably the numerical effort in comparison with the algorithm used on *a priori* any systems.

Thus, the state equation Eq.(1.a) is expressed as follows:

$$C_{apa}^{1/2} . C_{apa}^{1/2} \; \dot{T} = A_0 \, T + B_0 \, U \tag{2}$$

The change of variables, $\theta = C_{apa}^{1/2} . T$, is then applied. The system Eq.(1) is expressed as follows:

$$\begin{cases} \dot{\theta}(t) = A.\theta(t) + B.U(t) \\ Y(t) = C.\theta(t) + D.U(t) \end{cases} \tag{3}$$

where : $A = C_{apa}^{-1/2}. A_0 . C_{apa}^{-1/2} \, , \; B = C_{apa}^{-1/2} . B_0 \, , \; C = C_0 . C_{apa}^{-1/2}$

It is noticeable that the equality in transposed between the excitation and the observation matrices is still checked. This balance would have been broken by multiplying on the left each element of the Eq.(1.a) by the matrix C_{apa}^{-1} as it is usually done. Besides, the state

matrix A is symmetric contrarily to the matrix $C_{apa}^{-1}.A_0$ and has the same eigenvalues (these two matrices are real and strictly negative). The diagonalization of A leads to the modal form Eq.(4).

$$\begin{cases} \dot{X}_t = W.X_t + \Gamma.U_t \\ Y_t = H.X_t + D.U_t \end{cases} \tag{4}$$

The differential equations are then uncoupled and can be solved separately. An eigenvalue λ_i is associated with each eigenvector set in P such as $W = P^{-1}.A.P = diag\ (\lambda_i)$. The Eq.(2), based on the properties of the thermal conduction systems leads to the basic following relation concerning the matrix of base change : $\quad P^{-1} = P^T$.

This symmetric modal form reduces the calculation times due to the reversal of matrix P. Indeed, at first sight, calculation time is proportional to the cube of the matrix dimension. For a PC Pentium 32 Mo (133 MHz), the calculation time of the eigenvalues of a full matrix of order n can be highlight as follows : CPU Time=$7,50.10^{-6}.(n)^3$. With an adapted to symmetric matrix algorithm, this computing time can be decreased to : CPU Time = $2,90.10^{-6}.(n)^3$. Moreover, it allows to get rid of numerical problems linked to the reversal of big size matrices.

The control matrix Γ and the observation matrix H are expressed as follows:

$$\Gamma = P^T.C_{apa}^{-1/2}.B_0 \quad \text{and} \quad H = C_0.C_{apa}^{-1/2}.P \tag{5}$$

This enables to keep, the relation of equality between these two matrices : $\Gamma^T = H$.

The general algorithm of Moore allows to determine the r state variables which are considered as preponderant for the evolution of the model. Their evolution is deeply influenced by the excitations (they are the most controllable) and the transmission of their effects to the observed variables is important (the most observable). The gramians of controllability Wc and of observability Wo are two matrices which quantify these two notions. They are related to the state variables of systems such as Eq.(1) and Eq.(3). They are solutions to Lyapunov's equations Eq.(6) and are defined as positive.

$$A.Wc + Wc.A^T = -B.B^T \quad \text{and} \quad A^T.Wo + Wo.A = -C^T.C \tag{6}$$

The matrix Wc evaluates the influence of the control U on each state variable X. As for the matrix Wo, the influence of each state variable on the observation Y can be defined.

The first step of Moore's method consists in seeking a particular formulation of the original system such as the gramians are equal and diagonal: $Wc = Wo = \Sigma = diag(\sigma_1, ... \sigma_n)$.

In this new base, the state variables are thus as much controllable as observable. The matrix Π enabling to achieve this balanced base is called balancing transform.

A robust algorithm of the determination of Π has been developed in the field of automatic and control (Moore, 1981): determination of the gramians Wc and Wo – Choleski's decomposition of one of them $Wo = R^T.R$ – unitary diagonalization of the matrix $R^T.Wc.R$ into $V^T.\Sigma^2.V$ with $V^T.\ V = I$ and $\Sigma = diag(\sigma_1, ..., \sigma_n)$ such as $\sigma_1 \geq ... \geq ... \ \sigma_n$ – determination of the transformed matrix $\Pi = \Sigma^{-1/2}.\ V^T.\ R$.

The number of stages is relatively important when the system dealt with is *a priori* without peculiar property concerning control and observation. Moreover, numerical problems can be seen (Safonov & Chianga, 1989) if some variables are very weakly controllable and weakly observable (matrix Π can be numerically singular). Otherwise, the properties of the systems that we handle combined with the various simple processing presented above allow to reach an already balanced formulation Eq.(3). However, the gramians are equal but nondiagonal. Indeed, the control and observation matrices Γ and H being equal in transposed, gramians are equal Eq.(7) : $Wc = Wo$.

$$Wc_{ij} = -\frac{\sum_{m=1}^{q} \Gamma_{mi}.\Gamma_{mj}}{(\lambda_i + \lambda_j)} \quad \text{and} \quad Wo_{ij} = -\frac{\sum_{k=1}^{p} H_{ik}.H_{jk}}{(\lambda_i + \lambda_j)} \tag{7}$$

The determination of the balancing transform, such as defined by Moore, becomes immediate through an unitary diagonalization of one of the two gramians: $Wc = \Pi^T. \Sigma .\Pi$, with $\Pi^T.\Pi = I$ (identity matrix).

The expression of the balanced estimator is thus easily achieved compared to the general algorithm. The formulation of the system Eq.(3) in the new base ($\xi = \Pi.X$) is :

$$\begin{Bmatrix} \dot{\xi}_1 \\ \dot{\xi}_2 \end{Bmatrix} = \begin{bmatrix} Ae_{11} & Ae_{12} \\ Ae_{21} & Ae_{22} \end{bmatrix} . \begin{Bmatrix} \xi_1 \\ \xi_2 \end{Bmatrix} + \begin{bmatrix} Be_1 \\ Be_2 \end{bmatrix} \cdot U \text{ and } Y = \begin{bmatrix} Ce_1 & Ce_2 \end{bmatrix} . \begin{Bmatrix} \xi_1 \\ \xi_2 \end{Bmatrix} + [D] \cdot U \tag{8}$$

The r prevailing state variables are contained in the vector ξ_1. They are identified from the r biggest singular values $\Sigma_1 = diag(\sigma_1, ... , \sigma_r)$. r is determined in a recurrent way: a limit is established (99 % of the total sum of singular values). Beyond this limit, the contribution of the state variables (which are associated with $\Sigma_2 = diag(\sigma_{r+1}, ... , \sigma_n)$) to the behavior of the model is considered as negligible.

The elimination of the (n-r) weakest controllable and observable variables is then carried out by truncation (Ménézo, 1999). However, the static rate between the detailed model Eq.(8) and the reduced one Eq.(9) is preserved.

$$\begin{cases} \dot{\xi}_1 = \left(Ae_{11} - Ae_{12}.Ae_{22}^{-1}.Ae_{21} \right) \cdot \xi_1 + \left(Be_1 - Ae_{12}Ae_{22}^{-1}.Be_2 \right) \cdot U \\ \tilde{Y}(t) = \left(Ce_1 - Ce_2.Ae_{22}^{-1}.Ae_{21} \right) \cdot \xi_1 + \left(D - Ce_2.Ae_{22}^{-1}.Be_2 \right) \cdot U \end{cases} \tag{9}$$

3. COUPLING WITH THE OTHER PHENOMENA

3.1 Studied domain

In order to illustrate the efficient behavior of the reduced models, the modelling of a monozone cell is realised. This experimental cell, CIRCE (Fig. 2) belongs to the CoSTIC (Technique and Science Committee of Climatic Industries). A detailed description of the cell as well as the used metrology are to be found in the work of Palenzuela (1993).

The north wall is equipped with a simple glazing. Each wall is in contact with a climatic caisson which regulate the outside ambiences. The cell is equipped with an air change system. The supply takes place on the glazing and the exhaust on the opposite wall at the floor level. The measurements concern two kinds of heat emitter with very different dynamical characteristics : a heating floor (Fig. 3) and an electrical convector (EC).

The scenarios of the tests have been carried out on a period of 10 days. They have been designed in order to get a dynamic rate by modifying by steps : the climatic caisson temperatures, the air supply conditions (air supply flow Q_{sup} and air temperature T_{sup}). For the heating floor (HF), that was supplemented by steps imposed on the temperature of the coolant fluid. For the electrical convector (EC), controlled by a regulator, a modification of the control temperature on the inner air (Ta) has enabled us to get very quick variations on the convective injected power, P_{conv} (W).
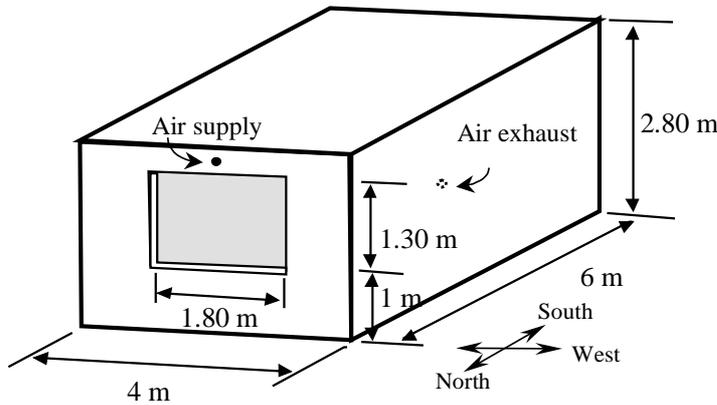
Figure 2- Dwelling cell
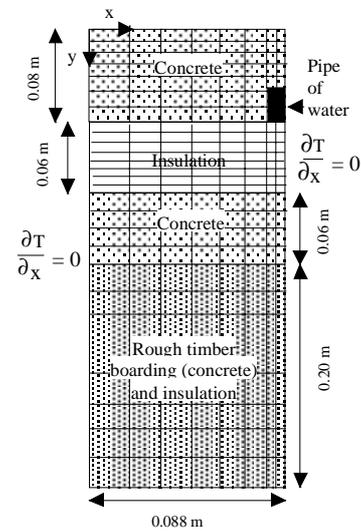
Figure 3- Elementary frame of the heating floor

The walls have been discretized in 1D, except for the floor (2D). Its decomposition into 68 elementary frame (Fig. 3) is defined from the symmetries of the spatial distribution of the draining network. The reduced models associated with the envelope components (Table 1) are coupled to each other by non-linear internal radiation and to the air volume by convection.

Table 1. Detailed and reduced orders of the envelope components

Model	North Wall	Glazing	West Wall	East Wall	South Wall	Heating floor	Ceiling
Detailed: n	10	1	10	10	10	196	10
Reduced : r	2	1	2	2	2	7	2

3.2 Coupling of the reduced order models

The cell is monozone and is not exposed to solar radiation. Consequently, heat transfer within this cell is characterized by : convection, long wavelength radiation (Φ_{net}) and conduction (Φ_{cond}). External boundary conditions of the envelope are the surface temperatures obtained from a data file (Dirichlet's conditions).

$$\Phi_{cond} + \Phi_{net} + S.hci.(Ta - Tsi) = 0 \tag{10}$$

The Eq.(10) represents the energetic balance at the inner surface of each component. The radiative heat exchanges between the walls of the cell are non linear (laws in Tsi^4). The determination of the net radiant fluxes (Φ_{net}) of each wall enables to carry out the coupling between the components of the envelope.

Superficial convection exchanges are the result of complex phenomena. We characterize the convection by a coefficient hci. According to the expected accuracy on the results, this coefficient is considered as constant or empirically related to a non-linear law such as Eq.(11). They are depending upon the gap between the surface temperature of the wall Tsi and the air temperature Ta. Coefficients a, b and m are issued from studies in natural convection and depend on both the wall orientation and the direction of the convective flux (Inard *et al.*, 1996).

$$hci = a\ |Tsi - Ta|^m + b \qquad (\text{W/m}^2.\text{K}) \tag{11}$$

These convective heat exchanges allows to couple the envelope (i.e. the set of conduction models of the envelope) with the air volume. In most of codes dedicated to building physics, this air volume is considered as isothermal (Ta). It enables to express the energetic balance of the air volume as follows :

$$(\rho a.ca.va).\dot{T}a = Q_{sup}.\rho a.ca.(T_{sup} - Ta) - \sum_{k=1}^{Np} (\Phi_{conv})_k + P_{conv} \tag{12}$$

The iterative calculation is first, simultaneously carried out from the balances on the air volume Eq.(12) and the inner faces of the envelope components. Below a given convergence limit, the resolution time step of the conductive systems Eq.(9) is incremented. This numerical coupling technique, of *ping-pong* type, enables to take into account non-linear exchange laws for convection and radiation (Ménézo, 1998).

4. Comparison with the experiments

All the simulations have been carried out in taking into account heat convective exchanges by an exchange coefficient hci for each wall. For each emitter, these coefficients have, first of all, been considered as constant (issued from the French Thermal Standard). A second serie of simulations has been carried out from empirical correlations Eq.(11) listed by Ménézo (1999).

The first category of results are concerning the heating floor (HF). Results reported on Fig.4 represent the evolution of the air temperature by taking into account constant exchange coefficients for each wall.
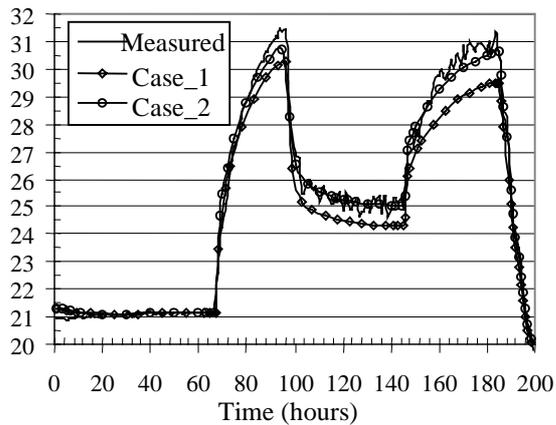
Figure 4- HF : Mean air temperature Ta (°C)
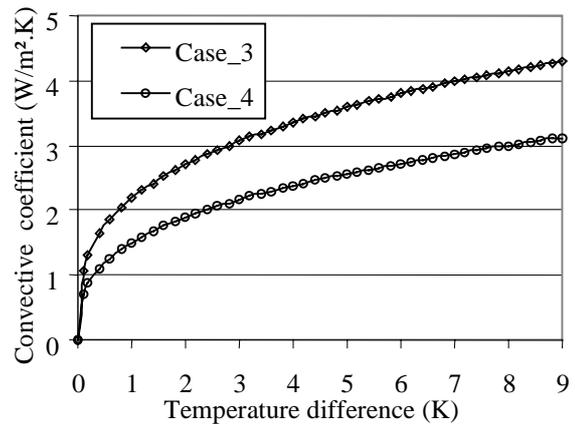
Figure 5- HF : Values of *hci* with 2 correlations

The two cases presented here correspond to two different values of this coefficient for the inner surface of the heating floor (Case_1 : *hci* = 3 W/m^2.K and Case_2 : *hci* = 4 W/m^2.K). We can notice that this coefficient is a very sensitive parameter for the model. The results of Case_2 are quite satisfactory as the discrepancy between the model (resulting from the assembling of the reduced order models) and the measurements doesn't exceed 0.5°C, during the second step imposed on the heating fluid temperature.

Simulations have been carried out from 2 non-linear laws describing convective exchanges (Fig.5) at the inner surface of the heating floor (Case_3 and Case_4). They result from experimental studies on that kind of heat source and are found in literature. The results are reported in Fig.6 for the air temperature and Fig.7 for the surface temperature of the floor. The uncoupling of the model responses appears after the first step imposed on the coolant fluid temperature. This sequence is characterised by an important difference between the floor surface temperature and the air temperature (about 7°C). Considering the observed scattering on the correlations (Fig.5), these gaps are not ascribable to the reduced conductive models.
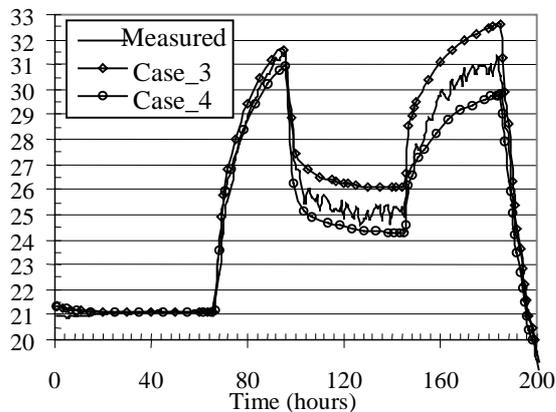
Figure 6- Mean air temperature Ta (°C)
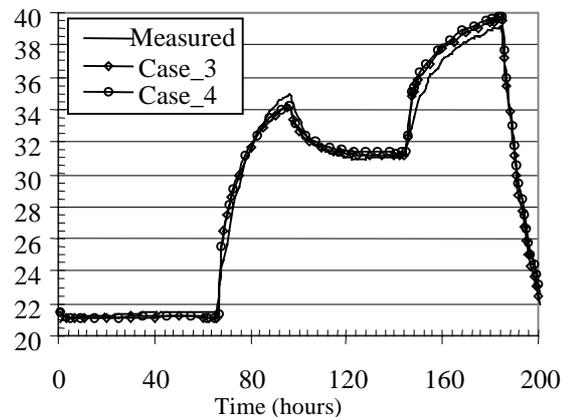
Figure 7- Floor surface mean Temperature (°C)

An intermediate empirical correlation, enabling us to improve noticeably the results, is possible. It is noticeable that the experimental conditions are extreme. In practice, the surface temperature of the floor is limited to 28°C for comfort reasons. This would normally lead to the reduction of the gaps noticed between simulations and the measurements.

The second category of results are concerning the electrical convector (EC). The results related to the evolution of the air temperature are shown in Fig.8. Case_1 has been carried out with invariant convective coefficients for each wall and Case_2 from non-linear empirical correlations.
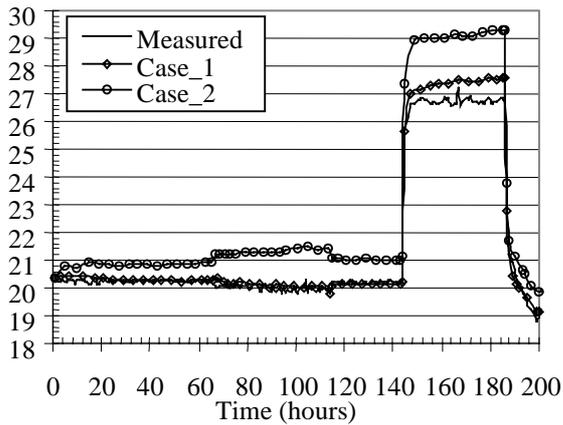
Figure 8- EC: Mean air temperature *Ta* (°C)
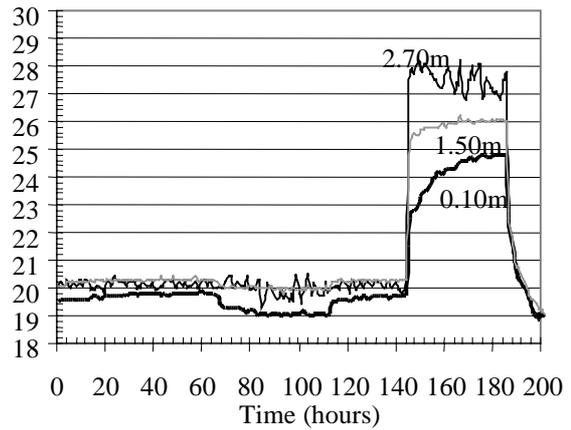
Figure 9- EC : Mesured air temperature *Ta* at different level of the cell (°C)
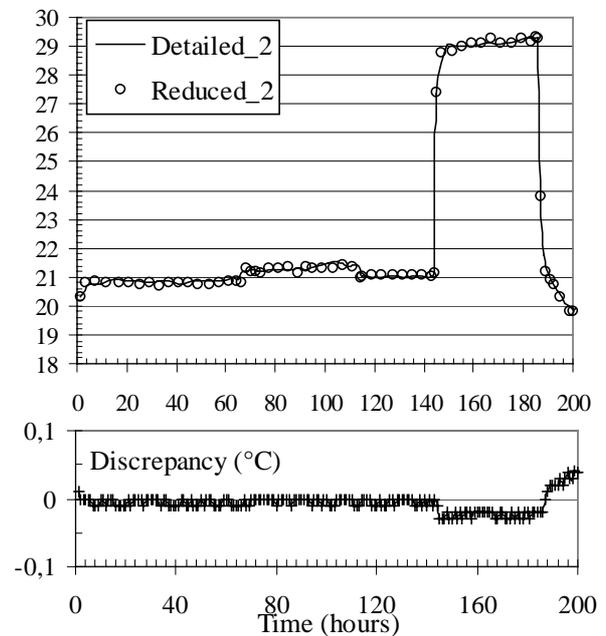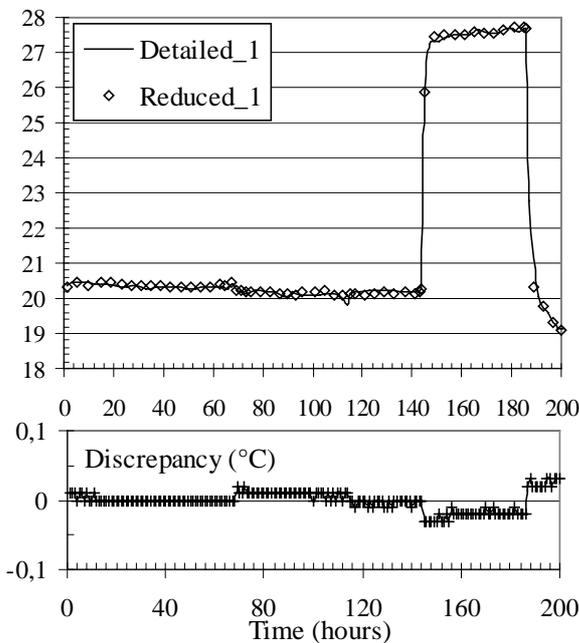
Figure 10- Discrepancies between the assemblings of detailed models and of reduced models (Case_1 and Case_2)

The evolution calculated in Case_1 is both qualitatively and quantitatively satisfactory in term of prediction of the mean air temperature. However, the results obtained with variable convective coefficients highlight the limits of an isothermal modelling of the air volume for a localized emission of heat. It is indeed characterized by an important heterogeneity of the temperature field within the cell (Fig.9). The behavior of the assembled reduced conduction models is very satisfactory and steady in comparison with the assembling of detailed models. Indeed, we have shown (Ménézo, 1999) that, for this dynamically penalizing configuration (emission of very unsteady convective power), the discrepancies don't exceed 0.05°C between these two models (Fig.10).

5. CONCLUSION

The algorithm suggested by Moore has been developed to deal efficiently with linear systems of any shape. The algorithm, suggested here and built on subsequent coupling considerations, limits the steps of the reduction technique. Indeed, obtaining the gramians equality, even before any treatment, enables to limit the numerical handling for the determination of the balancing transformation. The reduced models produced by this method, have a very stable dynamical behavior (mainly at the level of transient rates) experimentally confirmed.

However, we once more notice that the hypothesis of an isothermal air volume is too restrictive. The latter is however used by most of codes in the field of building physics. We are now working on the coupling of reduced order models with more accurate mass transfer models such as zonal models (Inard *et al.*, 1996). The principle of these models is to divide air volume into isothermal macro-volumes in order to evaluate fields of pressure and temperature in the air. The coupling of these two complementary approaches (zonal and reduction) aims at homogenising the modelling level of their respective domains (air volume and envelope). The first results are encouraging, in term of accuracy of results and numerical effort to provide.

REFERENCES

Inard, C., Bouia, H. & Dalicieux, P., 1996, Prediction of air temperature distribution in buildings with a zonal model. Energy and Buildings, vol 24, n° 2, pp. 125-132.

Ménézo, C., 1999, Contribution à la modélisation du comportement thermique des bâtiments par couplage de modèles réduits, Ph.D. diss., INSA of Lyon, France, 260 p.

Ménézo C., Castanet, S. & J.J. Roux, 1998, Simulation of heat transfer in buildings using reduced models coupled with non linearities, Proceedings of the 11th International Heat Transfer Conference, August 23-28, Taylor & Francis, Kyongju, Korea, Vol. 4, pp. 343-348.

Moore, B.C., 1981, Principal Component Analysis in Linear Systems: Controllability, Observability, and Model Reduction. IEEE Trans. on Contr., Vol. AC-26, n° 1, pp. 17-32.

Palenzuela, D., 1993, GREC : Etalonnage de la cellule d'essais CIRCE, CoSTIC, Digne, France

Safonov, G. &. Chianga, R.Y., 1989, Schur Method for Balanced-Truncation Model Reduction. IEEE Trans. on Contr., Vol. 34, n° 7, pp. 729-733